Do gait and muscle activation patterns change at middle-age during split-belt adaptation?

Vervoort, Danique; den Otter, Rob; Buurke, T J W; Vuillerme, Nicolas; Hortobagyi, Tibor; Lamoth, Claudine

Published in:
Journal of biomechanics

DOI:
10.1016/j.jbiomech.2019.109510

Publication date:
2020

Journal of Biomechanics 99 (2020) 109510

Contents lists available at ScienceDirect

Journal of Biomechanics

journal homepage: www.elsevier.com/locate/jbiomech
www.JBiomech.com

Do gait and muscle activation patterns change at middle-age during split-belt adaptation?

D. Vervoort [a,b,*], A.R. den Otter [a], T.J.W. Buurke [a], N. Vuillerme [b,c], T. Hortobágyi [a], C.J.C. Lamoth [a]

[a] University of Groningen, University Medical Center Groningen, Center for Human Movement Sciences, Groningen, The Netherlands
[b] University Grenoble-Alpes, AGEIS, Grenoble, France
[c] Institut Universitaire de France, Paris, France

ARTICLE INFO

Article history:
Accepted 12 November 2019

Keywords:
Split-belt walking
Gait adaptation
Muscle activation patterns
Middle-aged adults
Statistical Parametric Mapping

ABSTRACT

Advancing age affects gait adaptability, but it is unclear if such adaptations to split-belt perturbations are already affected at middle-age. Changes in neuromuscular control, that already start at middle-age, may underlie the age-related changes in gait adaptation. Thus, we examined the effects of age on adaptations in gait and muscle activation patterns during split-belt walking in healthy young and middle-aged adults. Young (23.3 ± 3.13 years) and middle-aged adults (55.3 ± 2.91 years) walked on an instrumented split-belt treadmill. Both age groups adapted similarly by reducing asymmetry in step length and double support time. Surface EMG was recorded from eight leg muscles bilaterally. Principal Component Analysis (PCA) was applied to the EMG data of all subjects, for the fast and slow leg separately, to identify muscle activation patterns. The principal components consisted of i.e. temporal projections that were analyzed with Statistical Parametric Mapping (SPM). The functional muscle groups, identified by PCA, increased activation during early adaptation and post-adaptation, and decreased activation over time similarly in both age groups. Extra activation peaks of the plantar- and dorsiflexors suggest a role in gait modulation during split-belt walking. Both young and middle-aged adults re-established gait symmetry and showed adaptation effects in the muscle activation patterns. Since the adaptation of muscle activation patterns parallels adaptation of gait symmetry, changes in muscle activation likely underlie the changes in step parameters during split-belt adaptation. In conclusion, split-belt adaptation, in terms of gait and muscle activation patterns, is still preserved at middle-age, suggesting that age-related differences occur later in the lifespan.

1. Introduction

Advancing chronological age reduces the ability to adapt to changes in the environment (McCrum et al., 2016). Preserving gait adaptability seems crucial in preventing adverse outcomes, such as falls (Lurie et al., 2013; Pai et al., 2014). The nature of why, and at what age gait adaptability becomes compromised remains unclear.

A popular paradigm to examine gait adaptability is split-belt walking, where gait is perturbed by imposing asymmetric belt speeds (Reisman et al., 2005). Directly after the belt speed perturbation, step length and double support time become asymmetric. After several minutes, symmetry is re-established through bilateral adjustments in these variables (Buurke et al., 2018; Malone and Bastian, 2010; Reisman et al., 2005).

Data on age-related changes in split-belt adaptations so far have been inconsistent. Step length symmetry remained unaffected by age in some studies (Malone and Bastian, 2016; Roemmich et al., 2014; Vervoort et al., 2019), while others reported age-effects on adaptation rate of step length symmetry (Bruijn et al., 2012; Sombric et al., 2017). If age effects exist, its underlying mechanism may relate to modifications in timing and amplitude of muscle activation. Immediately after the split-belt perturbation, leg muscle activation increases, and then decreases as adaptation progresses (Finley et al., 2013; MacLellan et al., 2014). Also, changes in stance times were associated with an earlier onset and higher amplitude of m. gastrocnemius activation in the fast leg, higher m. tibialis anterior activation in the slow leg and higher m. tibialis anterior - m. gastrocnemius co-activation in the slow leg (Dietz et al., 1994). While these individual muscles show adaptations to split-belt walking, when faced with adaptive challenges, different

* Corresponding author at: University of Groningen, University Medical Center Groningen, Center for Human Movement Sciences, Antonius Deusinglaan 1, 9713 AV Groningen, The Netherlands.
E-mail address: d.vervoort@umcg.nl (D. Vervoort).

https://doi.org/10.1016/j.jbiomech.2019.109510
0021-9290/

neuromuscular control strategies could operate. Assessment of such strategies involves the identification of functional muscle groups, muscles that are activated simultaneously and generate specific movements, which are controlled by a common activation pattern that allows the central nervous system to simplify neuromuscular control (Ivanenko et al., 2006). These strategies can be measured with EMG.

Using pattern recognition methods, young adults' split-belt gait was previously characterized by four activation patterns. A temporal shift to 3–4% earlier in the gait cycle was observed in two uni- and bilateral activation patterns, likely due to changes in gait cycle timing (MacLellan et al., 2014). Split-belt walking causes an asymmetry in muscle activation, which may be most accurately reflected by unilateral activation patterns. The control strategies of each leg could be autonomous, but the ipsilateral leg needs to interact with the contralateral leg to flexibly control walking and adapt to belt speed differences (Choi and Bastian, 2007).

At older age, these activation patterns might be affected differently, because age increases the level of co-activation between agonist-antagonist muscle pairs (Schmitz et al., 2009) and decreases the onset latency between the tibialis anterior and gastrocnemius muscles (Hortobágyi et al., 2009). Already during middle-age there are several neuromuscular changes that arguably affect muscle activation during split-belt walking. During the 5th decade of human life, muscle mass starts to decline by 1–2% per year (Muscaritoli et al., 2013) and leg muscle strength, muscle power, and muscle quality decline, respectively, by 0.7–0.9%, 1.2–1.9% and 1.5–2.4% per year (Kennis et al., 2014). As expected based on such structural changes in muscle size, maximal voluntary force of the quadriceps is 30% lower in middle-aged compared with young adults (Chuang et al., 2019). It is conceivable that changes in muscle activation patterns associated with split-belt perturbations are already present at middle-age. Detecting age-related differences in the ability to adapt to split-belt perturbations before gait adaptability is impaired, might help preserve gait adaptability with older age without the presence of other factors that could affect this relationship, like deconditioning or disease.

The aim of this study is to examine the effect of age on adaptations of gait and muscle activation patterns induced by split-belt walking. We hypothesize that even if gait adaptation to the split-belt perturbation is unaffected by age, its underlying neuromuscular control may still differ between age groups. We expect the muscle activation patterns to change over the course of adaptation, to modulate changes in gait cycle timing. The functional muscle groups will increase activation during early adaptation and post-adaptation. Finally, we hypothesize that middle-aged adults increase the activation and change the timing of functional muscle groups compared to young adults.

2. Methods

2.1. Participants

Eleven healthy young (23.3 ± 3.13 years, 5 females, BMI = 23.3 ± 2.93, hours participated in sports/week = 4.5 ± 3.10) and ten middle-aged adults (55.3 ± 2.91 years, 6 females, BMI = 23.1 ± 2.43, hours participated in sports/week = 4.1 ± 1.49) participated in this study. Participants could walk outdoors without aids and understand verbal instructions. Exclusion criteria were previous experience with split-belt walking, orthopedic surgery of the lower extremities in the last two years, and neurological disorders, psychiatric disorders and/or medication use that might affect postural control and gait. The study protocol was approved by the local Ethical Committee of the Center of Human Movement Sciences of the University Medical Center Groningen. All participants signed a written informed consent before participating.

2.2. Instrumentation and procedure

Participants walked on an instrumented split-belt treadmill (Motek, Amsterdam, The Netherlands). Embedded force plates measured ground reaction forces and center of pressure at 1000 Hz. Surface EMG was measured with a Trigno wireless system (bandwidth: 20-450 Hz; Delsys, Natick, MA, USA) at 2000 Hz on eight leg muscles bilaterally: Gluteus Medius (GM), Biceps Femoris (BF), Semitendinosus (ST), Rectus Femoris (RF), Vastus Medialis (VM), Medial Gastrocnemius (GAS), Soleus (SOL) and Tibialis Anterior (TA). Electrode placement locations were determined and prepared using SENIAM guidelines (Hermens et al., 1999).

During the split-belt protocol participants first walked tied-belt with a fast (1.4 m/s) and slow baseline (0.7 m/s). During adaptation, one belt was accelerated from 0.7 m/s to 1.4 m/s, while the other belt stayed at 0.7 m/s. Participants returned to tied-belt walking at 0.7 m/s during post-adaptation (Fig. 1). The fast and slow belts were randomly assigned per participant.

2.3. Data analysis

Data were analyzed off-line with custom-made Matlab algorithms (R2015b, MathWorks, Natick, MA, USA). Force plate data were recursively filtered with a 15 Hz second-order low-pass Butterworth filter. Gait events were determined when the vertical ground reaction forces crossed the 50 N threshold. Gait parameters were averaged over the first and last five steps of each phase, late slow baseline (BL), early adaptation (EA), late adaptation (LA), early post-adaptation (EP) and late post-adaptation (LP).

EMG data were high-pass filtered using a 30 Hz second-order Butterworth filter, full-wave rectified using an absolute Hilbert transform, and low-pass filtered (10 Hz second-order recursive Butterworth filter). EMG data were down-sampled to 1000 Hz to obtain similar sample frequencies for the EMG and force plate data. EMG and force plate data were manually synchronized by aligning the moment of heel-strike of the left leg with the peak in TA EMG activation of the left leg.

EMG data were time normalized with 100 data points per gait cycle, 60 data points for the stance phase and 40 data points for the swing phase, starting at heel-strike (Den Otter et al., 2004). Amplitude normalization was done by dividing the EMG signal by the maximum amplitude of the fast baseline EMG for each individual muscle. EMG was averaged for the first (EA, EP) or last five strides of the phases (BL, LA, LP). EMG data of one young subject was not included in the analysis.

2.4. Gait parameters

Step Length (SL) was defined as the anterior-posterior distance between anteroposterior COP position of the left and right leg at

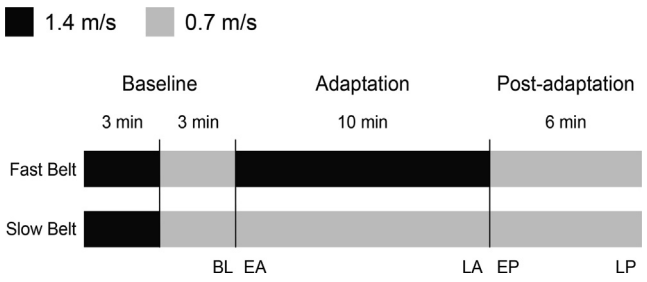

Fig. 1. Split-belt protocol. Healthy young and middle-aged adults walked on a split-belt treadmill with tied- and split-belt phases. During the split-belt phase, the fast and slow belt were randomly assigned to left or right per participant. Abbreviations: BL = late slow baseline, EA = early adaptation, LA = late adaptation, EP = early post-adaptation, LP = late post-adaptation.

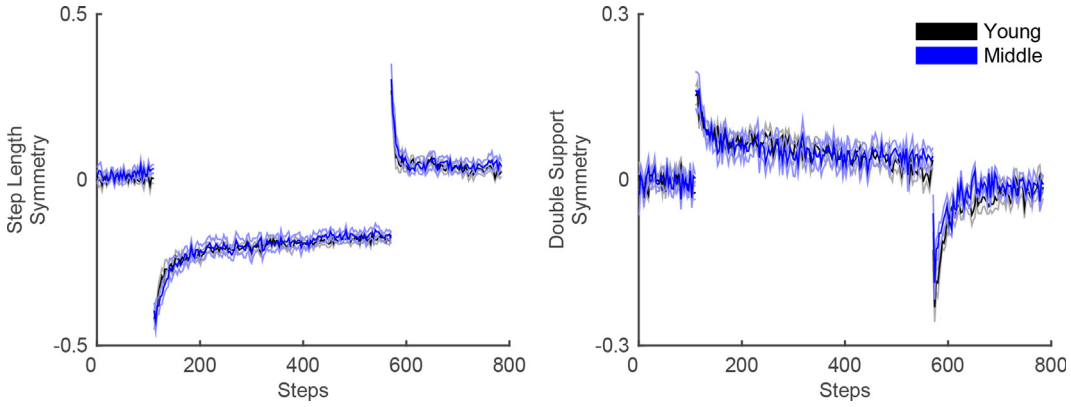

Fig. 2. Adaptation in step length and double support symmetry for young (black) and middle-aged adults (blue). Step length and double support symmetry are averaged over 3 steps and show the development over the entire split-belt protocol. For the figure, all phases consist of the lowest number of steps per phase, thus the baseline consists of 110 steps, the adaptation phase of 460 steps and the post-adaptation phase of 215 steps. (For interpretation of the references to colour in this figure legend, the reader is referred to the web version of this article.)

Table 1
The main effect of Phase and post-hoc testing for the gait parameters.

	Mean ± sd for the five phases					Main effect of Phase		
Gait parameters	BL	EA	LA	EP	LP	F-value	p-value	ES
SLS	0.01 ± 0.04	−0.41 ± 0.08	−0.16 ± 0.04	0.26 ± 0.13	0.02 ± 0.05	$F_{(2.03,39)}$ = 242.02	**<0.001**	**0.93**
DSS	0.00 ± 0.04	0.16 ± 0.06	0.02 ± 0.05	−0.14 ± 0.08	0.00 ± 0.04	$F_{(2.44,46)}$ = 74.91	**<0.001**	**0.80**
Post-hoc testing	*BL vs. EA*		*EA vs. LA*		*BL vs. EP*		*BL vs. LP*	
	$t_{(21)}$	p	$t_{(21)}$	p	$t_{(21)}$	p	$t_{(21)}$	p
SLS	25.29	**<0.001**	−12.21	**<0.001**	−8.10	**<0.001**	−1.52	0.14
DSS	−10.61	**<0.001**	7.94	**<0.001**	7.83	**<0.001**	−0.42	0.68

The table presents results of the repeated measures ANOVA (phase effect) and the post-hoc *t*-test comparisons between phases, with the F/t-values (F/t(df)) and the p-values. Gait parameter values of the five tested phases are given with mean ± standard deviation. P-values are highlighted in bold if the phases were significantly different (after Holm-Bonferroni correction). Abbreviations: BL = late slow baseline; EA = early adaptation; LA = late adaptation; EP = early post-adaptation; LP = late post-adaptation; SLS = step length symmetry; DSS = double support symmetry; ES = effect size.

contralateral toe-off (Buurke et al., 2018). Double Support time (DS) was defined as the time both feet were in contact with the ground, with the fast DS starting at heel-strike of the fast leg (Reisman et al., 2005). Symmetry for SL (SLS) and DS (DSS) was calculated as:

$$Symmetry(i) = \frac{Fast(i) - Slow(i)}{Fast(i) + Slow(i)}$$

2.5. Principal component analysis

Principal Component Analysis (PCA) was applied to study differences in amplitude or timing of the overall muscle activation pattern, by reducing the original individual EMG signals to a lower number of principal components (PCs) (Daffertshofer et al., 2004).

The input in the PCA was the combined EMG data of all phases and all participants, for the fast and slow leg separately. For each participant, an EMG matrix ($X_{m,c}$) was created by concatenating the phases (c) of each muscle (m). Then all subjects were included in one matrix (X_{EMG}; formulas see Appendix).

Based on X_{EMG}, the covariance matrix was estimated. The eigenvectors and eigenvalues were calculated and sorted in descending order of eigenvalues. The temporal projections were determined by projecting the original EMG data onto the eigenvectors (Appendix). The number of PCs was established using the eigenvalue spectrum, with as cut-off criterion the gap between eigenvalues on a log-log scale (Daffertshofer et al., 2004).

2.6. Statistical analysis

2.6.1. Gait parameters

Two repeated measures ANOVAs were performed for the dependent variables SLS and DSS, with within-subjects factor Phase (BL, EA, LA, EP, LP) and between-subjects factor Group (young vs. middle-aged adults). Post-hoc testing was done with dependent t-tests with Holm-Bonferroni correction for the Phase comparisons: BL vs. EA (effect of perturbation), EA vs. LA (adaptive change), BL vs. EP (aftereffects) and BL vs. LP (return to baseline). Statistical analysis was performed in SPSS 24.0 (IBM, Armonk, NY, USA). Level of significance was set at $p < 0.05$.

2.6.2. Statistical parametric mapping on PCA outcomes

The temporal projections of the PCs were analyzed with Statistic Parametric Mapping (SPM). SPM uses random field theory to make statistical inferences regarding time series data (see Friston et al., 1995; Pataky, 2010; Pataky et al., 2013).

In SPM, test statistics are calculated for every data point of the time series to obtain a statistical parametric map. Based on the temporal gradients, the temporal smoothness of the SPM trajectory is estimated (Penny et al., 2011). A critical threshold is calculated using random field theory, so only 5% (α) of the smooth random trajectory is expected to cross this threshold. These supra-threshold clusters correspond to time frames where statistically significant effects are detected. For each supra-threshold cluster an individual probability (p) value is calculated (Cao and Worsley, 1999). Occasionally small supra-threshold clusters (<5% of cycle) are detected that are less likely to contain meaningful information. These clusters are reported in Table 3, but not discussed in the text.

The temporal projections were the input in the repeated measures ANOVA SPM, with within-subjects factor Phase (BL, EA, LA, EP, LP) and between-subjects factor Group (young vs. middle-aged). Post-hoc testing was done with an SPM *t*-test with Bonferroni correction, for the phase comparisons: BL vs. EA, EA vs.

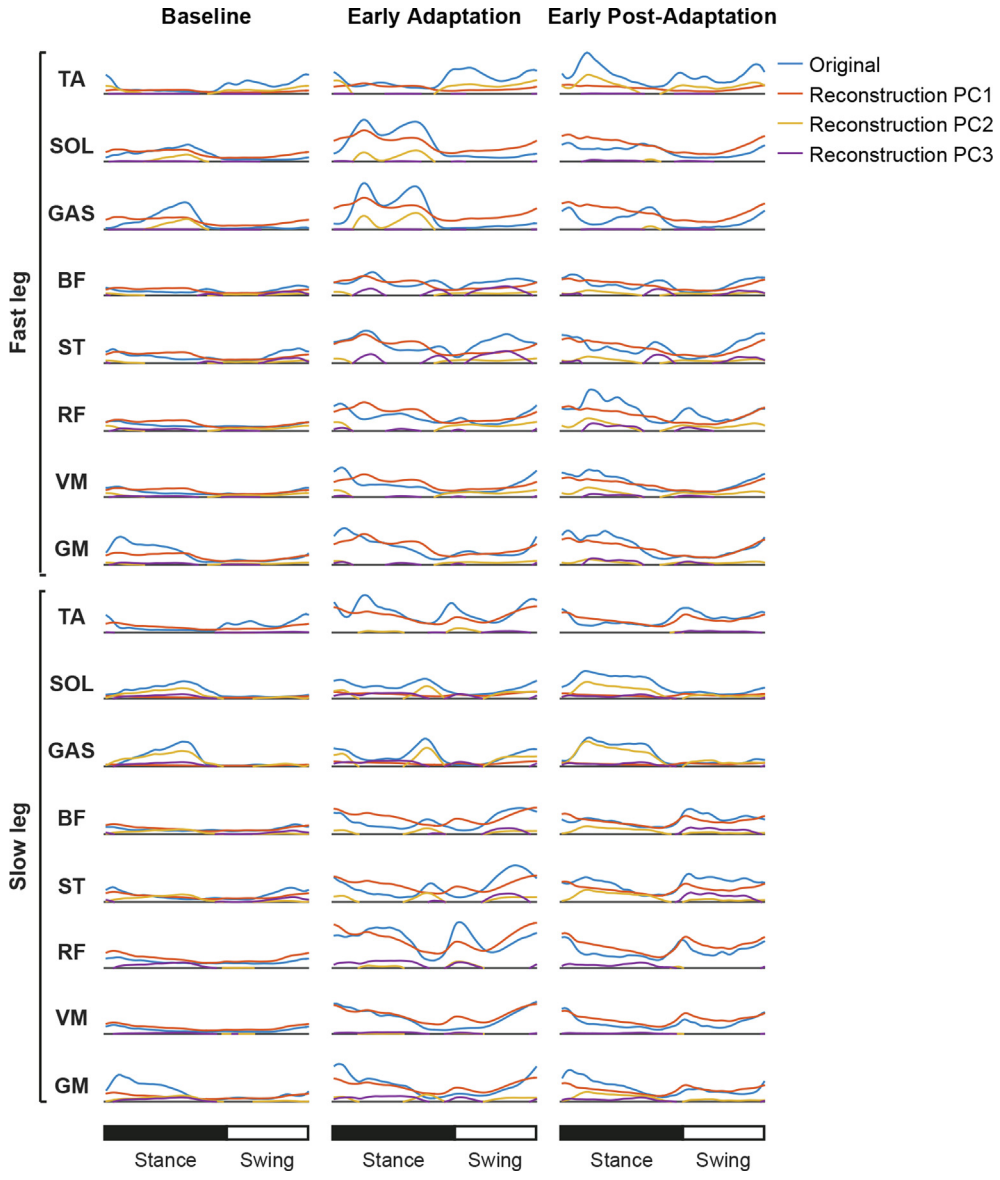

Fig. 3. EMG profiles and reconstructions of PC1-3 for all muscles during baseline, early-adaptation, and post-adaptation. The original EMG signal (blue) is shown next to the signals that were reconstructed from the temporal projections and eigenvectors of the PCs as follows: $X_{rec}(j) = \sum V_m(j) * Y_k(j)$ (Daffertshofer et al., 2004). The reconstructions show which part of the original EMG signal is captured within each PC. The data of all subjects are pooled since there were no group differences. Abbreviations: TA = Tibialis Anterior; SOL = Soleus; GAS = Gastrocnemius Medialis; BF = Biceps Femoris; ST = Semitendinosus; RF = Rectus Femoris; VM = Vastus Medialis; GM = Gluteus Medius. (For interpretation of the references to colour in this figure legend, the reader is referred to the web version of this article.)

Table 2
Eigenvectors of all 8 muscles for the three PCs of the fast and slow leg. The muscles that contribute to that PC are highlighted (>0.25).

	Fast leg			Slow leg		
Muscles	*PC1*	*PC2*	*PC3*	*PC1*	*PC2*	*PC3*
TA	0.14	**0.49**	0.03	**0.35**	**0.26**	0.11
SOL	**0.42**	**0.41**	0.09	0.09	**0.43**	**0.31**
GAS	**0.42**	**0.60**	0.01	0.07	**0.63**	**0.30**
BF	**0.27**	0.13	**0.51**	**0.35**	0.20	**0.43**
ST	**0.38**	0.17	**0.66**	**0.35**	**0.31**	**0.61**
RF	**0.38**	**0.32**	**0.40**	**0.60**	**0.38**	**0.38**
VM	**0.31**	0.25	0.16	**0.39**	0.05	0.08
GM	**0.41**	0.13	**0.34**	**0.32**	0.25	**0.29**

Abbreviations: TA = Tibialis Anterior; SOL = Soleus; GAS = Gastrocnemius Medialis; BF = Biceps Femoris; ST = Semitendinosus; RF = Rectus Femoris; VM = Vastus Medialis; GM = Gluteus Medius.

LA, BL vs. EP and BL vs. LP. The SPM analyses were performed in Matlab with open-source spm1d code (version M.0.1, www.spm1d.org).

3. Results

3.1. Gait parameters

The effect of Phase was significant for SLS and DSS. Post-hoc testing revealed that SLS and DSS showed asymmetry in EA, with a negative asymmetry for SLS (larger steps of the fast leg), and a positive asymmetry for DSS (larger double support times of the slow leg; see Fig. 2 and Table 1). This asymmetry leveled out towards LA, and the aftereffects in EP are in the opposite direction, i.e. a positive SLS and a negative DSS (see Fig. 2 and Table 1). No group effects were found.

3.2. Muscle activation patterns

Results of the PCA for the fast and slow leg revealed three PCs, explaining ±77% of data's variance. Fig. 3 illustrates the reconstruction of the EMG signal, based on the temporal projections and eigenvectors of the individual PCs. These reconstructions show which part of the original EMG signal is captured by each PC. The reconstruction of all PCs together shows that three PCs represent the original EMG signal well (Appendix Fig. A1). The PCs of the fast leg explained respectively 37.1%, 26.7%, and 12.5%, and the PCs of the slow leg explained 43.1%, 19.3%, and 15.1%. The associated eigenvectors of the muscles are presented in Table 2.

3.2.1. SPM analysis

Table 3 shows the results of the SPM {F} and post-hoc SPM {t} tests on the temporal projections of the three extracted PCs. For the fast leg, the projections of all three PCs showed an effect of Phase. For the slow leg, the projection of the first and second PC showed an effect of Phase. No group or interaction effects were found.

3.2.2. Post-hoc SPM comparison across phases

Fig. 4 shows the post-hoc test for the effect of phase for PC1 of the fast and slow leg, with the temporal projections of the phases (first and third row of graphs) and the SPM results of the post-hoc comparison between phases (second and fourth row). Post-hoc testing for PC1 of the fast leg showed increased activation in EA compared to BL and LA (Table 3; Fig. 4). During EA, there was an extra peak around 15% of the gait cycle, related to the extra activation peaks of the GAS, SOL, BF, ST (Fig. 3). These muscles could be activated to stabilize the leg while suddenly moving at a faster speed. Muscle activation during EP was significantly larger compared to BL. LP did not significantly differ from BL, suggesting a complete return to normal walking.

Table 3
Results of the SPM {F} and post-hoc SPM {t} tests on the temporal projections of the fast (top panel) and slow leg (bottom panel).

		PC1			*PC2*			***PC3***		
SPM	*DF*	*CT*	*Supra-threshold clusters*	*p-values*	*CT*	*Supra-threshold clusters*	*p-values*	*CT*	*Supra-threshold clusters*	*p-values*
Fast leg										
Phase	F(4,72)	4.48	1) 0–69.4%	**p < 0.001**	4.76	1) 6.0–43.7%	**p < 0.001**	4.89	*1) 59.5–62.8%*	*p = 0.02*
			2) 72.8–100%	**p < 0.001**		2) 52.2–65.3%	**p < 0.001**		2) 71.0–82.3%	**p < 0.001**
						3) 82.4–84.5%	*p = 0.039*			
EA vs. BL	t(1,38)	3.83	1) 0–100%	**p < 0.001**	3.90	*1) 0–4.1%*	*p = 0.003*	3.92	1) 12.0–21.0%	**p < 0.001**
						2) 10.6–17.8%	**p < 0.001**		2) 69.4–82.8%	**p < 0.001**
						3) 40.4–44.5%	*p = 0.003*			
						4) 53.0–100%	**p < 0.001**			
LA vs. EA	t(1,38)	3.83	*1) 0–2.6%*	*p = 0.009*	3.88	1) 52.8–82.4%	**p < 0.001**	3.92	*1) 15.5–19.7%*	*p = 0.003*
			2) 7.1–83.7%	**p < 0.001**					2) 69.5–81.7%	**p < 0.001**
			3) 95.6–100%	*p = 0.005*						
EP vs. BL	t(1,38)	3.83	1) 0–66.2%	**p < 0.001**	3.94	1) 7.4–41.1%	**p < 0.001**	3.96	1) 13.8–19.2%	**p < 0.001**
			2) 76.5–100%	**p < 0.001**		2) 53.8–65.6%	**p < 0.001**		*2) 44.4–45.6%*	*p = 0.011*
						3) 79.5–95.5%	**p < 0.001**		3) 59.1–64.3%	**p < 0.001**
LP vs. BL	t(1,38)	3.89	–	–	3.94	–	–	3.92	–	–
Slow leg										
Phase	F(4,72)	4.39	1) 0–100%	**p < 0.001**	4.75	1) 0–19.6%	**p < 0.001**	4.85	–	–
						2) 28.7–40.4%	**p < 0.001**			
						3) 45.1–51.4%	**p = 0.005**			
						4) 95.5–100%	*p = 0.017*			
EA vs. BL	t(1,38)	3.78	1) 0–100%	**p < 0.001**	3.85	*1) 0–3.4%*	*p = 0.006*	–	–	–
						2) 12.4–39.0%	**p < 0.001**			
						3) 44.5–51.4%	**p < 0.001**			
						4) 57.5–67.5%	**p < 0.001**			
						5) 94.7–100%	**p = 0.002**			
LA vs. EA	t(1,38)	3.79	1) 0–100%	**p < 0.001**	3.85	*1) 0–4.3%*	*p = 0.004*	–	–	–
						2) 15.3–19.3%	*p = 0.005*			
						3) 24.3–38.3%	**p < 0.001**			
						4) 44.1–52.5%	**p < 0.001**			
						5) 59.2–67.3%	**p < 0.001**			
						6) 95.2–100%	*p = 0.003*			
EP vs. BL	t(1,38)	3.76	1) 0–90.8%	**p < 0.001**	3.93	1) 6.8–21.6%	**p < 0.001**	–	–	–
			2) 91.1–100%	**p < 0.001**		2) 63.5–76.2%	**p < 0.001**			
LP vs. BL	t(1,38)	3.79	–	–	3.95	–	–	–	–	–

The table presents results of the repeated measures SPM {F} analysis (phase effect) and the post-hoc SPM {t} tests, with the F/t-values (F/t(df)), the critical threshold, the supra-threshold clusters, and the p-values. The p-values of the clusters that are discussed in the text are highlighted in bold. Small supra-threshold clusters and p-values that likely do not represent meaningful results are given in italic. Abbreviations: DF = degrees of freedom, CT = critical threshold; BL = late slow baseline; EA = early adaptation; LA = late adaptation; EP = early post-adaptation; LP = late post-adaptation.

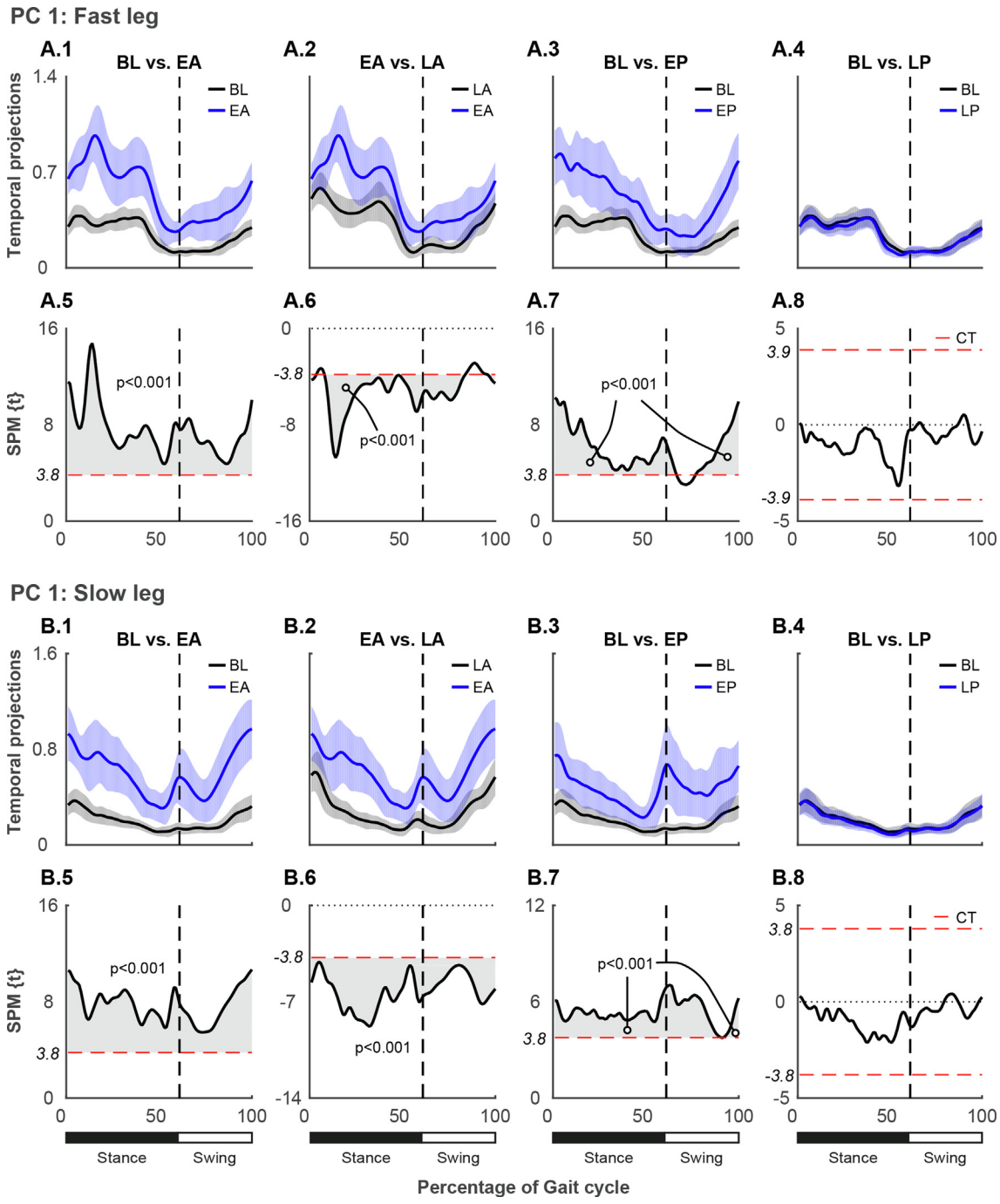

Fig. 4. Post-hoc SPM t-tests (SPM {t}) for PC1 of the fast (A) and slow leg (B), showing the changes in temporal projections across phases of the split-belt protocol. For both panels, the upper graphs (1–4) show the temporal projections of the phases that are compared to each other, with the SPM {t} results of that comparison shown in the graphs below (5–8). A larger temporal projection shows an increase in overall muscle activation, while a lower temporal projection shows a decrease in overall muscle activation. At a corrected level of $\alpha = 0.013$, the red dotted line indicates the critical threshold of significance. The vertical black dotted line shows the stance (0–60%) and swing phase (60–100%). Abbreviations: BL = late slow baseline, EA = early adaptation, LA = late adaptation, EP = early post-adaptation, LP = late post-adaptation, CT = critical threshold. (For interpretation of the references to colour in this figure legend, the reader is referred to the web version of this article.)

Similar effects were seen for PC1 of the slow leg (Table 3). During EA, muscle activation was significantly higher than BL and LA, and had an extra peak around 60% of the gait cycle (Fig. 4). During EP, muscle activation was significantly higher and had an extra peak around 60% compared to BL. The extra peak at 60% was related to the peak in RF and TA activation (Fig. 3). Possibly, the slow leg requires more control during swing initiation. LP and BL did not differ significantly.

Fig. 5 shows the post-hoc test for the effect of phase for PC2 of the fast and slow leg, with the temporal projections of the phases (first and third row of graphs) and the SPM results of the post-hoc comparison between phases (second and fourth row). Post-hoc testing for PC2 of the fast leg showed significantly increased activation during EA compared to BL (53.0–100%; Table 3; Fig. 5), and an extra activation peak (10.6–17.8%), due to GAS and SOL activation (Fig. 3). Muscle activation during EA was significantly higher than

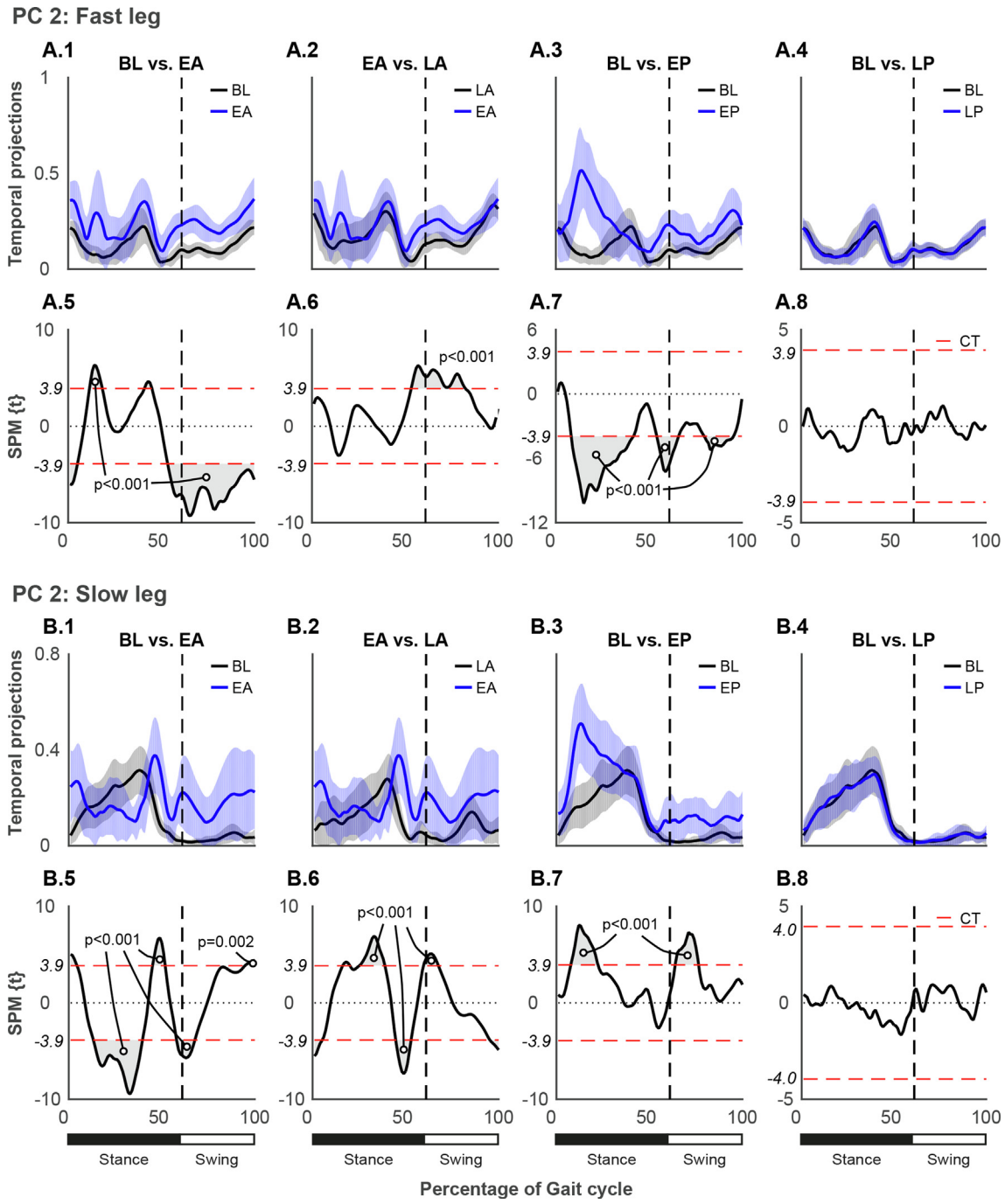

Fig. 5. Post-hoc SPM t-tests (SPM {t}) for PC2 of the fast (A) and slow leg (B), showing the changes in temporal projections across phases of the split-belt protocol. For both panels, the upper graphs (1–4) show the temporal projections of the phases that are compared to each other, with the SPM {t} results of that comparison shown in the graphs below (5–8). A larger temporal projection shows an increase in overall muscle activation, while a lower temporal projection shows a decrease in overall muscle activation. At a corrected level of $\alpha = 0.013$, the red dotted line indicates the critical threshold of significance. The vertical black dotted line shows the stance (0–60%) and swing phase (60–100%). Abbreviations: BL = late slow baseline, EA = early adaptation, LA = late adaptation, EP = early post-adaptation, LP = late post-adaptation, CT = critical threshold. (For interpretation of the references to colour in this figure legend, the reader is referred to the web version of this article.)

LA (52.8–82.4%). Two supra-threshold clusters showed increased activation in EP compared to BL (53.8–65.6%, 79.5–95.5%), while the other cluster showed an extra activation peak (7.4–41.1%), which is likely due to TA activation during the stance phase. LP did not significantly differ from BL.

For PC2 of the slow leg, EA differed from BL with decreased activation from 12.4 to 39.0% of the gait cycle, a delayed activation peak from 44.5 to 51.4% and increased activation from 57.5 to 67.5% (Table 3; Fig. 5). Muscle activation was significantly lower in EA compared to LA from 24.3 to 38.3% of the gait cycle, had a delayed peak from 44.1 to 52.5%, and an extra peak from 59.2 to 67.3%. EP significantly differed from BL during stance with an extra burst (6.8–21.6%) and increased activation (63.5–76.2%) likely associated with GAS and SOL activation (Fig. 3). LP and BL did not differ significantly.

Post-hoc testing for PC3 of the fast leg showed supra-threshold clusters with increased activation in EA compared to BL (12.0–21.0%, 69.4–82.8%) and LA (69.5–81.7%; Table 3), due to BF and

ST activation (Fig. 3). During EP, two small clusters showed increased activation compared to BL (13.8–19.2%, 59.1–64.3%). LP and BL did not differ significantly.

4. Discussion

We studied the effects of age on adaptations of gait and muscle activation patterns induced by split-belt walking. Young and middle-aged adults adapted step lengths and double support times to split-belt walking. The functional muscle groups, identified by PCA, increased activation during early adaptation and post-adaptation, and decreased activation over time. The adaptations in these patterns might contribute to the restoration of step symmetry during split-belt adaptation. Contrary to our hypothesis, both age groups adapted gait features as well as muscle activation patterns in a similar way during all phases of split-belt walking.

In agreement with previously reported data, split-belt walking modified walking, and both age groups decreased asymmetry in step length and double support time during adaptation (Buurke et al., 2018; Finley et al., 2013; Reisman et al., 2005). There are mixed results on the effects of age on gait adaptation with regards to gait symmetry, with some studies reporting age-related decline in step length symmetry (Bruijn et al., 2012; Sombric et al., 2017) and others reporting no effects (Roemmich et al., 2014; Vervoort et al., 2019). We extend this literature by showing that middle-aged adults exhibited similar (de-)adaptations as young adults, suggesting that gait adaptability remains intact in middle-age. The mixed results could be due to differences between studies in subject characteristics, split-belt conditions, and data analysis. To reduce the inconsistencies, future studies should examine how gait adaptations evolve across the lifespan using uniform methods. Such an approach could determine which outcome is the most sensitive to detect the onset of slow or aberrant adaptation caused by natural aging.

Although gait adaptation is not different at middle-age, the underlying neuromuscular control might be different. We, however, found that adaptations in muscle activation to split-belt walking were also independent of age. During early adaptation, the first activation pattern showed increased activation, followed by a decrease in activation as adaptation progressed. The decrease in muscle activation over the course of adaptation was previously suggested to parallel the decrease in gait asymmetry and thus show a more efficient gait pattern (Finley et al., 2013; MacLellan et al., 2014). Similar adaptation effects are seen in platform perturbation studies, with increased muscle activation in response to unexpected perturbations, which decreased with repetitions of the perturbation (Horak et al., 1989; Oude Nijhuis et al., 2009). In the current study, the decrease in muscle activation with adaptation parallels the decrease in gait asymmetry. Since muscle activation reflects the neural drive, we suggest that changes in activation patterns underlie the changes in gait during the adaptation process.

Plantarflexors and dorsiflexors emerged as key functional regulators of adaptation to split-belt walking. These muscle groups were involved in the modulation of gait cycle timing during split-belt (de-)adaptation. A unique adaptive role for the plantarflexors and dorsiflexors was previously identified during split-belt walking (Dietz et al., 1994). The plantarflexors provide push-off power (Neptune et al., 2001), regulate step length (Varraine et al., 2000), and contribute to restraining falls (Honeine et al., 2013). During normal walking, aging increases (co-)activation of agonist-antagonist muscles, e.g. the plantarflexors and dorsiflexors (Hortobágyi et al., 2009; Schmitz et al., 2009). This change in muscle (co-)activation might affect the ability of older adults to modulate gait during split-belt walking.

One possible reason for a lack of age effects is that the locomotor challenge created by these speeds of split-belt walking were insufficient in proportion to the level of neuromuscular dysfunction at middle-age in terms of muscle strength and quality (Kennis et al., 2014; Muscaritoli et al., 2013). It is also possible that the neuromuscular changes at middle-age are not large enough to cause differences, because the adaptive responses needed are well within the neuromuscular reserve present at middle-age.

If split-belt adaptation is within the neuromuscular reserve at middle-age, this places the split-belt paradigm between some other paradigms that test dysfunction in adaptability. Middle-aged adults were able to adapt their margin of stability to perturbed walking with an ankle strap resistance (McCrum et al., 2016), but needed more recovery steps to adapt (Süptitz et al., 2013). During a slip and fall protocol, middle-aged adults experienced slightly more falls than younger adults, but generally could recover quite similarly (Lockhart et al., 2005). Middle-aged adults also had delayed muscle activation peaks compared to young adults during platform perturbations (de Freitas et al., 2010). Thus, while the continuous perturbation of split-belt walking does not show any aging effects at middle-age, these perturbation models with sudden, short perturbations show some small signs of dysfunction of adaptability. That could indicate that the split-belt paradigm appears to be at the easier end of the perturbation continuum for middle-aged adults.

In the current study, we used a task-specific maximum peak amplitude value for the EMG amplitude normalization. This method is an alternative to MVIC-based normalization of EMG data (Burden, 2010). With this method, we created an EMG template of the specific task, i.e., walking, used frequently in locomotion studies (Finley et al., 2013; MacLellan et al., 2014; Schmitz et al., 2009). Such normalization of EMG activity does not affect timing of muscle activation but could reduce age-differences in the magnitude of activation.

5. Conclusions and recommendations

Adaptations in gait and muscle activation patterns during split-belt walking are still preserved at middle-age. Both young and middle-aged adults re-established gait symmetry and showed adaptations in the muscle activation patterns. Since the adaptations in muscle activation patterns parallel the adaptation of gait symmetry, changes in muscle activation likely underlie the changes in step parameters during split-belt adaptation. Future studies should consider using a lifespan approach to examine gait and muscle activation adaptations to split-belt perturbations. This will provide information about when advancing age starts to affect adaptability in terms of gait and muscle activation, which could form a basis for fall prevention interventions and suggested target groups with aging.

Acknowledgements

We would like to thank Linda Wolthuizen and Tessa Huisjes for their help during the measurements, Lotte Knol and Timon Louwsma for their help with the manual synchronization, and Wim Kaan, Dirk van der Meer and Emyl Smid for their technical support. Lastly, we would like to thank the participants.

Author contributions

DV, NV, TH, and CL designed the study protocol. DV collected and analyzed the data with supervision of CL. Results were inter-

preted by DV, AR, TB, NV, TH, and CL. DV wrote the first draft under supervision of CL, and DV, AR, TB, NV, TH, and CL contributed significantly to revising the manuscript. All authors read and approved the final manuscript.

Declaration of competing interest

The authors declare that they have no conflict of interest.

Funding

There are no sources of funding to declare.

Availability of data and material

The data set used and analyzed in the current study is available from the corresponding author on reasonable request.

Appendix.

Principal component analysis (PCA)

The concatenated EMG matrix ($X_{m,c}$) of one participant consists of 100 data points per phase (k) of all 5 phases (c) of 8 muscles (m) = 500 samples of 8 muscles.

$$X_{m,c} = \left(\begin{pmatrix} X_{1,1} & \cdots & X_{1,k} \\ \vdots & \cdots & \vdots \\ X_{m,1} & \cdots & X_{m,k} \end{pmatrix}_1 \cdots \begin{pmatrix} X_{1,1} & \cdots & X_{1,k} \\ \vdots & \cdots & \vdots \\ X_{m,1} & \cdots & X_{m,k} \end{pmatrix}_c \right)$$

The final EMG matrix for the PCA analysis consists of all included participants, with k (100 samples) * c (5 phases) * p (20 participants) = 10,000 samples of 8 muscles ($X_{8,10000}$).

$$X_{EMG} = \left((X_{m,c})_1 \cdots (X_{m,c})_p \right)$$

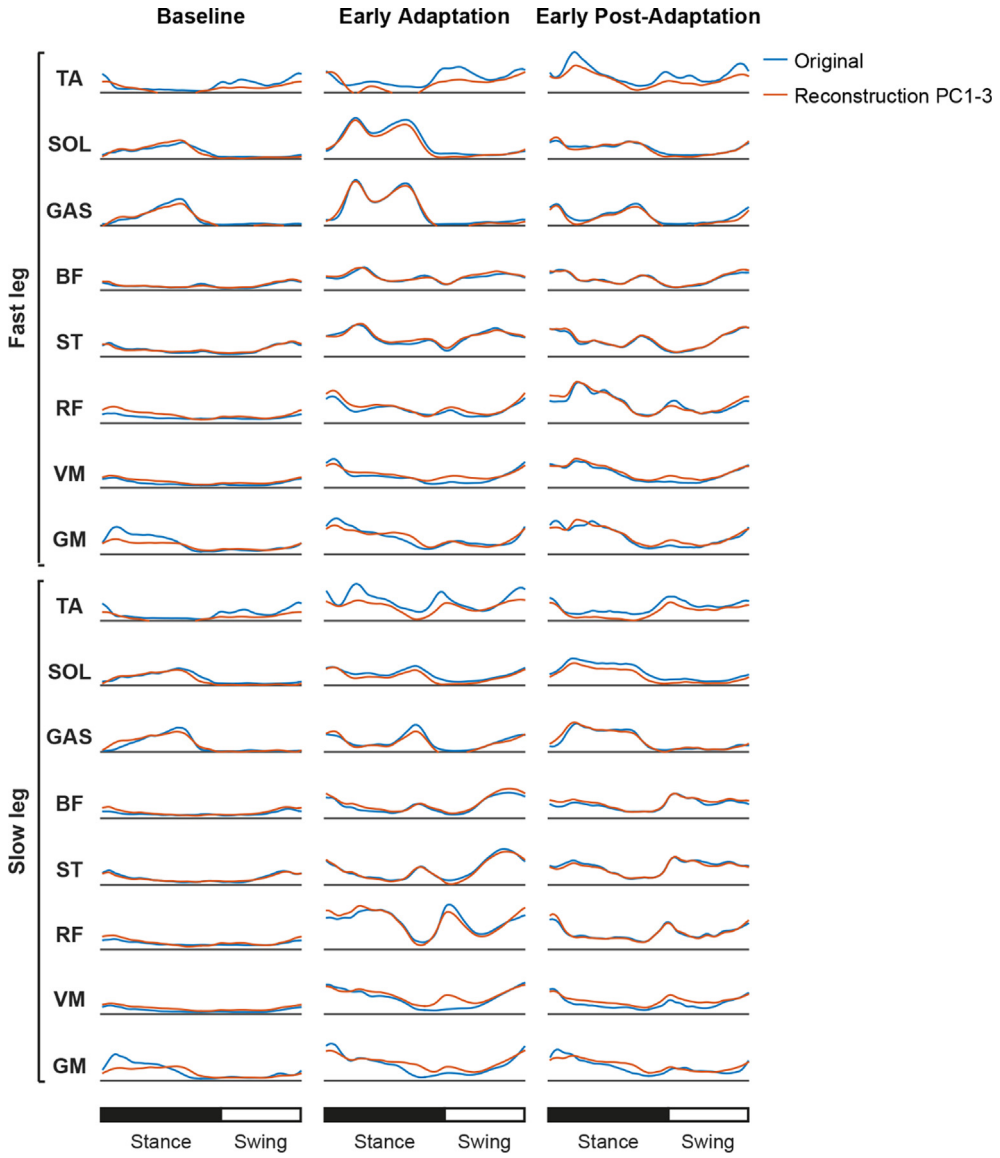

Fig. A1. EMG profiles and the reconstruction of the PCs for all muscles during baseline, early-adaptation, and post-adaptation. The original EMG signal (blue) is shown next to the signal that was reconstructed (red) from the temporal projections and eigenvectors of the PC as follows: $X_{rec} = \sum_{j=1}^{3} V_m(j) * Y_k(j)$ (Daffertshofer et al., 2004). The data of all subjects are pooled since there were no group differences. Abbreviations: TA = Tibialis Anterior; SOL = Soleus; GAS = Gastrocnemius Medialis; BF = Biceps Femoris; ST = Semitendinosus; RF = Rectus Femoris; VM = Vastus Medialis; GM = Gluteus Medius.

Based on the EMG matrix ($X_{8,10000}$), the covariance matrix can be defined as (Daffertshofer et al., 2004):

$Cov_X = \frac{1}{N-1}\sum_{i=1}^{N}\left(X_{m,i} - \bar{X_m}\right)\left(X_{k,i} - \bar{X_k}\right)$ with $\bar{X_m} = \frac{1}{N}\sum_{i=1}^{N} X_{m,i}$.

With N as the number of samples and i as the sample.

Based on the covariance matrix, the eigenvectors (V) and eigenvalues (λ) of each PC (j) are determined (Daffertshofer et al., 2004).

$D = V * V^{-1} * Cov_X$ with $D_{jk} = \lambda_j$ for $j = k$

With D as the diagonal matrix of eigenvalues (λ). The eigenvalues show the amount of variance of the original data set that is explained by a specific PC. The eigenvector of each PC is build up by m muscles, with the n^{th} eigenvector representing the amount that that specific muscle contributed to that PC. If the eigenvector value exceeds 0.25, that muscle is important for that PC.

The temporal projections (Y) were determined by projecting the original EMG set (X) onto the eigenvectors (V) (Daffertshofer et al., 2004).

$$Y_k^{(j)} = \sum_{m=1}^{16} V_m^{(j)} * X_{m,k}$$

References

Bruijn, S.M., Van Impe, A., Duysens, J., Swinnen, S.P., 2012. Split-belt walking: adaptation differences between young and older adults. J. Neurophysiol. 108, 1149–1157. https://doi.org/10.1152/jn.00018.2012.

Burden, A., 2010. How should we normalize electromyograms obtained from healthy participants? What we have learned from over 25 years of research. J. Electromyogr. Kinesiol. https://doi.org/10.1016/j.jelekin.2010.07.004.

Buurke, T.J.W., Lamoth, C.J.C., Vervoort, D., Van der Woude, L.H.V., Den Otter, A.R., 2018. Adaptive control of dynamic balance in human gait on a split-belt treadmill. J. Exp. Biol. 221, jeb174896. https://doi.org/10.1242/jeb.174896.

Cao, J., Worsley, K.J., 1999. The detection of local shape changes via the geometry of Hotelling's T^2 fields. Ann. Stat. 27, 925–942. https://doi.org/10.1214/aos/1018031263.

Choi, J.T., Bastian, A.J., 2007. Adaptation reveals independent control networks for human walking. Nat. Neurosci. 10, 1055–1062. https://doi.org/10.1038/nn1930.

Chuang, Y.-F., Chen, C.-C., Hsu, M.-J., Huang, N.-J., Huang, Y.-Z., Chan, H.-L., Chang, Y.-J., 2019. Age related changes of the motor excitabilities and central and peripheral muscle strength. J. Electromyogr. Kinesiol. 44, 132–138. https://doi.org/10.1016/j.jelekin.2018.12.007.

Daffertshofer, A., Lamoth, C.J.C., Meijer, O.G., Beek, P.J., 2004. PCA in studying coordination and variability: a tutorial. Clin. Biomech. 19, 415–428. https://doi.org/10.1016/j.clinbiomech.2004.01.005.

de Freitas, P.B., Knight, C.A., Barela, J.A., 2010. Postural reactions following forward platform perturbation in young, middle-age, and old adults. J. Electromyogr. Kinesiol. 20, 693–700. https://doi.org/10.1016/j.jelekin.2009.11.009.

Den Otter, A.R., Geurts, A.C.H., Mulder, T., Duysens, J., 2004. Speed related changes in muscle activity from normal to very slow walking speeds. Gait Post. 19, 270–278. https://doi.org/10.1016/S0966-6362(03)00071-7.

Dietz, V., Zijlstra, W., Duysens, J., 1994. Human neuronal interlimb coordination during split-belt locomotion. Exp. Brain Res. 101, 513–520. https://doi.org/10.1007/BF00227344.

Finley, J.M., Bastian, A.J., Gottschall, J.S., 2013. Learning to be economical: the energy cost of walking tracks motor adaptation. J. Physiol. 591, 1081–1095. https://doi.org/10.1113/jphysiol.2012.245506.

Friston, K.J., Holmes, A.P., Worsley, K.J., Poline, J., Frith, C.D., Frackowiak, R.S.J., 1995. Statistical parametric maps in functional imaging: a general linear approach. Hum. Brain Mapp. 2, 189–210. https://doi.org/10.1002/hbm.460020402.

Hermens, H.J., Freriks, B., Merletti, R., Stegeman, D., Blok, J., Rau, G., Disselhorst-Klug, C., Hägg, G., 1999. European recommendations for surface electromyography. Roessingh Res. Develop.

Honeine, J.-L., Schieppati, M., Gagey, O., Do, M.-C., 2013. The functional role of the triceps surae muscle during human locomotion. PLoS ONE 8,. https://doi.org/10.1371/journal.pone.0052943 e52943.

Horak, F.B., Diener, H.C., Nashner, L.M., 1989. Influence of central set on human postural responses. J. Neurophysiol. 62, 841–853. https://doi.org/10.1152/jn.1989.62.4.841.

Hortobágyi, T., Solnik, S., Gruber, A., Rider, P., Steinweg, K., Helseth, J., DeVita, P., 2009. Interaction between age and gait velocity in the amplitude and timing of antagonist muscle coactivation. Gait Post. 29, 558–564. https://doi.org/10.1016/j.gaitpost.2008.12.007.

Ivanenko, Y.P., Poppele, R.E., Lacquaniti, F., 2006. Motor control programs and walking. Neuroscientist 12, 339–348. https://doi.org/10.1177/1073858406287987.

Kennis, E., Verschueren, S., Van Roie, E., Thomis, M., Lefevre, J., Delecluse, C., 2014. Longitudinal impact of aging on muscle quality in middle-aged men. Age (Omaha) 36, 9689. https://doi.org/10.1007/s11357-014-9689-1.

Lockhart, T.E., Smith, J.L., Woldstad, J.C., 2005. Effects of aging on the biomechanics of slips and falls. Hum. Factors 47, 708–729. https://doi.org/10.1518/001872005775571014.

Lurie, J.D., Zagaria, A.B., Pidgeon, D.M., Forman, J.L., Spratt, K.F., 2013. Pilot comparative effectiveness study of surface perturbation treadmill training to prevent falls in older adults. BMC Geriatr. 13, 49. https://doi.org/10.1186/1471-2318-13-49.

MacLellan, M.J., Ivanenko, Y.P., Massaad, F., Bruijn, S.M., Duysens, J., Lacquaniti, F., 2014. Muscle activation patterns are bilaterally linked during split-belt treadmill walking in humans. J. Neurophysiol. 111, 1541–1552. https://doi.org/10.1152/jn.00437.2013.

Malone, L.A., Bastian, A.J., 2016. Age-related forgetting in locomotor adaptation. Neurobiol. Learn. Mem. 128, 1–6. https://doi.org/10.1016/j.nlm.2015.11.003.

Malone, L.A., Bastian, A.J., 2010. Thinking about walking: effects of conscious correction versus distraction on locomotor adaptation. J. Neurophysiol. 103, 1954–1962. https://doi.org/10.1152/jn.00832.2009.

McCrum, C., Epro, G., Meijer, K., Zijlstra, W., Bruggemann, G.P., Karamanidis, K., 2016. Locomotor stability and adaptation during perturbed walking across the adult female lifespan. J. Biomech. 49, 1244–1247.

Muscaritoli, M., Lucia, S., Molfino, A., Cederholm, T., Fanelli, F.R., 2013. Muscle atrophy in aging and chronic diseases: is it sarcopenia or cachexia?. Intern. Emerg. Med. 8, 553–560. https://doi.org/10.1007/s11739-012-0807-8.

Neptune, R.R., Kautz, S.A., Zajac, F.E., 2001. Contributions of the individual ankle plantar flexors to support, forward progression and swing initiation during walking. J. Biomech. 34, 1387–1398.

Oude Nijhuis, L.B., Allum, J.H.J., Borm, G.F., Honegger, F., Overeem, S., Bloem, B.R., 2009. Directional Sensitivity of "first trial" reactions in human balance control. J. Neurophysiol. 101, 2802–2814. https://doi.org/10.1152/jn.90945.2008.

Pai, Y.-C., Bhatt, T., Yang, F., Wang, E., 2014. Perturbation training can reduce community-dwelling older adults' annual fall risk: a randomized controlled trial. Journals Gerontol. Ser. A 69, 1586–1594. https://doi.org/10.1093/gerona/glu087.

Pataky, T.C., 2010. Generalized n-dimensional biomechanical field analysis using statistical parametric mapping. J. Biomech. 43, 1976–1982. https://doi.org/10.1016/j.jbiomech.2010.03.008.

Pataky, T.C., Robinson, M.A., Vanrenterghem, J., 2013. Vector field statistical analysis of kinematic and force trajectories. J. Biomech. 46, 2394–2401. https://doi.org/10.1016/j.jbiomech.2013.07.031.

Penny, W.D., Friston, K.J., Ashburner, J.T., Kiebel, S.J., Nichols, T.E., 2011. Statistical parametric mapping: the analysis of functional brain images. Elsevier.

Reisman, D.S., Block, H.J., Bastian, A.J., 2005. Interlimb coordination during locomotion: what can be adapted and stored?. J. Neurophysiol. 94, 2403–2415. https://doi.org/10.1152/jn.00089.2005.

Roemmich, R.T., Nocera, J.R., Stegemöller, E.L., Hassan, A., Okun, M.S., Hass, C.J., 2014. Locomotor adaptation and locomotor adaptive learning in Parkinson's disease and normal aging. Clin. Neurophysiol. 125, 313–319. https://doi.org/10.1016/j.clinph.2013.07.003.

Schmitz, A., Silder, A., Heiderscheit, B., Mahoney, J., Thelen, D.G., 2009. Differences in lower-extremity muscular activation during walking between healthy older and young adults. J. Electromyogr. Kinesiol. 19, 1085–1091. https://doi.org/10.1016/j.jelekin.2008.10.008.

Sombric, C.J., Harker, H.M., Sparto, P.J., Torres-Oviedo, G., 2017. Explicit action switching interferes with the context-specificity of motor memories in older adults. Front. Aging Neurosci. 9, 40. https://doi.org/10.3389/fnagi.2017.00040.

Süptitz, F., Catalá, M.M., Brüggemann, G.P., Karamanidis, K., 2013. Dynamic stability control during perturbed walking can be assessed by a reduced kinematic model across the adult female lifespan. Hum. Mov. Sci. 32, 1404–1414. https://doi.org/10.1016/j.humov.2013.07.008.

Varraine, E., Bonnard, M., Pailhous, J., 2000. Intentional on-line adaptation of stride length in human walking. Exp. Brain Res. 130, 248–257. https://doi.org/10.1007/s002219900234.

Vervoort, D., den Otter, A.R., Buurke, T.J.W., Vuillerme, N., Hortobágyi, T., Lamoth, C. J.C., 2019. Effects of Aging and Task Prioritization on Split-Belt Gait Adaptation. Front. Aging Neurosci. 11, 10. https://doi.org/10.3389/fnagi.2019.00010.